

Organic cation dependent hot carrier relaxation dynamics in two-dimensional perovskites

Haoran Pang^{1,a,*}

¹*School of Physics and Optoelectronic Engineering, Guangdong University of Technology, Guangzhou, 510006, China*

^a*a13622203091@163.com*

**Corresponding author*

Abstract: Hot carrier solar cells (HCSC) have attracted extensive attention due to the efficient utilization of high-energy photons. Two-dimensional (2D) perovskites is one of the materials suitable as HCSC due to the hot phonon bottleneck effect as well as the quantum well structure. Providing methods to regulate the hot carrier cooling rate of 2D perovskites is crucial for further technological development. In this study, we systematically investigate the role of organic molecules in regulating hot carrier relaxation in 2D $n = 1$ perovskites through time-resolved spectroscopic measurements. The results of transient absorption and time-resolved photoluminescence reveal that hot carrier relaxation in 2D perovskites takes place on sub-picosecond time scales and can be effectively modulated by component engineering of organic molecules. These insightful results contribute to deep understanding of the hot carrier relaxation process of 2D perovskites and provide valuable information for the future development of higher performance perovskite solar cells.

Keywords: 2D perovskite; time-resolved spectra; hot carrier relaxation; component engineering

1. Introduction

Over the past decade or so, three-dimensional (3D) organic-inorganic hybrid perovskites have been extensively studied for their interesting and practical physical phenomena, such as band gap tunability,^[1,2] long carrier diffusion length^[3-5] and low trap state density.^[6] The power conversion efficiency (PCE) of 3D perovskite solar cells has witnessed a remarkable increase, which is close to the SQ limit of single-junction cells.^[7,8] However, the poor stability of 3D perovskites against oxygen and moisture greatly limits their commercial application. In contrast, two-dimensional (2D) layered perovskites, which incorporate organic molecules among inorganic layer, have superior stability.^[9-11] Organic molecules act as a protective layer, increasing the activation energy for ion migration and thus preventing the inorganic layer from being exposed to moisture and oxygen.^[12-14] However, the incorporation of organic layer with insulating properties results in a larger bandgap and poorer carrier transport characteristics, leading to a lower PCE in comparison to 3D perovskite solar cells.^[15,16]

In order to overcome the limitations of SQ theory and further improve the PCE of solar cells, the concept of hot carrier solar cells (HCSC) has been proposed.^[17] When high-energy photons excite semiconductors, hot carrier with excess energy are generated. Subsequently, hot electrons rapidly release the excess heat and relax to the bottom of the conduction band. The central theory of HCSC is to extract the excess energy from the hot carriers before the heat lost occurs, reducing the energy loss and thus enabling efficient utilization of short-wavelength solar radiation.^[18-22] However, the hot carrier relaxation process usually occurs in ultrafast time scales, making the extraction of energy very difficult. Due to the hot phonon bottleneck effect and the unique quantum well structure, 2D perovskites have a slower hot carrier cooling rate compared to other semiconductors, making them one of the suitable materials for HCSC.^[23-26] Slow hot carrier relaxation is the crucial key to HCSC, and providing methods to regulate the hot carrier cooling rate of 2D perovskites is essential for further technological development of HCSC. It has been reported that the hot carrier cooling rate of 3D perovskites can be efficiently regulated by component engineering (cations or halogen atoms),^[27-29] but there are fewer reports on the role of different organic molecules in regulating the hot carrier relaxation dynamics of 2D perovskites.

In this study, we comprehensive investigated the role of four widely used organic molecules (n-butylammonium (BA), phenethylammonium (PEA), 2-thiophenethylammonium (TEA), 2-thiophenemethylammonium (TMA)) in regulation the hot carrier relaxation process in 2D $n = 1$

perovskites via time-resolved spectroscopic techniques. Transient absorption (TA) and time-resolved photoluminescence (TRPL) experiments at the same excitation wavelengths demonstrate that hot carrier cooling occurs on a sub-picosecond time scales, with the order of the relaxation time generally following $(\text{PEA})_2\text{PbI}_4 > (\text{TEA})_2\text{PbI}_4 > (\text{BA})_2\text{PbI}_4 > (\text{TMA})_2\text{PbI}_4$. Our work reveals that hot carrier relaxation in 2D perovskites can be efficiently regulated through organic molecular component engineering, which provides important information for the further development of HCSC.

2. Results and discussion

2.1. Sample preparation and Steady state characterizations

We fabricated 2D perovskites using one-step spin-coating procedure described in Figure 1. The steady-state absorption spectra of the four samples are shown in Figure 2a, with the absorption peak around 520 nm corresponds to 2D $n=1$ perovskites.^[10] In order to minimize the influence of film thickness inconsistencies, we attempted to keep the absorption intensity of the four 2D perovskites as consistent as possible. Compared with $(\text{TMA})_2\text{PbI}_4$, the absorption peak of $(\text{TEA})_2\text{PbI}_4$ exhibited a gradual red shift. Figure 2b shows the steady-state photoluminescence (PL) spectra of the four samples, with the peak around 530 nm corresponding to the PL features of the 2D $n=1$ perovskite and no other peak observed.^[9] The PL signature of $(\text{TEA})_2\text{PbI}_4$ exhibited a slight red shift compared to $(\text{TMA})_2\text{PbI}_4$, which is consistent with the absorption spectra. Under the same absorption intensity and experimental conditions, we observed that the PL intensity of 2D perovskites was in the order of $(\text{PEA})_2\text{PbI}_4 > (\text{TEA})_2\text{PbI}_4 > (\text{TMA})_2\text{PbI}_4 > (\text{BA})_2\text{PbI}_4$, with the PL intensity of $(\text{PEA})_2\text{PbI}_4$ is approximately one order of magnitude larger than that of $(\text{BA})_2\text{PbI}_4$.

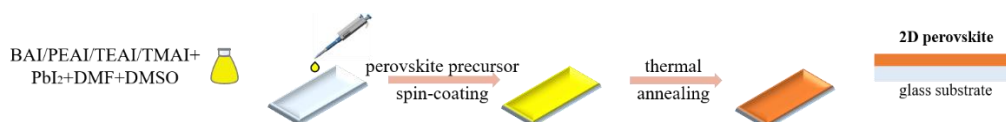


Figure 1: Schematic illustration of the 2D perovskite films fabrication process.

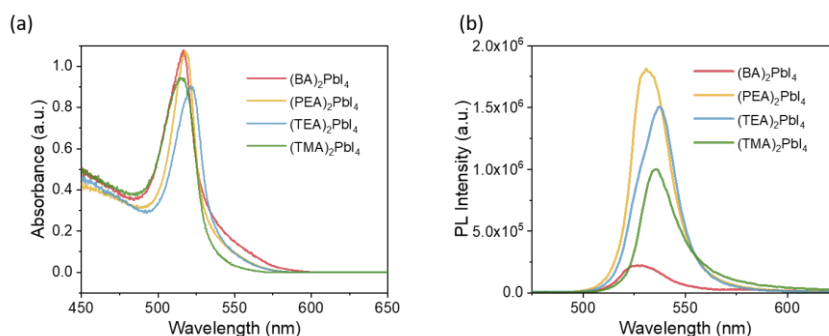


Figure 2: (a) Steady-state absorption spectra of 2D $n=1$ perovskites. (b) Steady-state PL spectra of 2D $n=1$ perovskites under excitation at 400 nm.

2.2. Transient absorption (TA) spectra

Transient absorption (TA) measurements were carried out on the four different 2D perovskites. Initially, a pump wavelength of 530 nm was utilized to near-resonant excite 2D perovskites. Under this excitation wavelength, the carrier will be excited to band edge of conduction without generation of hot carrier. The obtained TA spectra are presented at Figure 3 and showed similar features. All spectra exhibit a negative ground state bleaching (GSB) band at ~ 520 nm and a positive broad photoinduced absorption (PIA) band at ~ 500 nm. The positions of the GSB correspond to the steady-state absorption of 2D perovskites (Figure 2a).

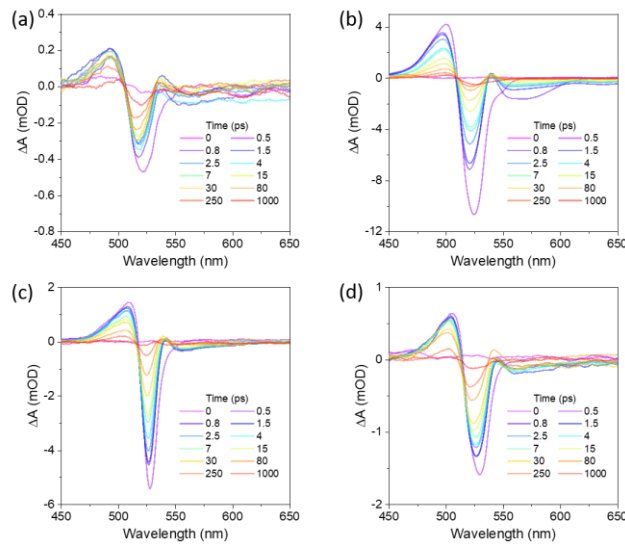


Figure 3: TA spectra under excitation at 530 nm of (a) $(\text{BA})_2\text{PbI}_4$, (b) $(\text{PEA})_2\text{PbI}_4$, (c) $(\text{TEA})_2\text{PbI}_4$ and (d) $(\text{TMA})_2\text{PbI}_4$ at different delay times.

To reveal the hot carrier relaxation dynamics of 2D perovskites, we performed TA measurements at pump wavelength of 400 nm. The excitation energy of 400 nm is considerably higher than bandgap of 2D perovskites (Figure 2a), which could result in hot carrier relaxation. Due to the fast time scale of hot carrier cooling to the band edge, we set equally spaced delay steps within the first 5 picosecond (ps) and logarithmic steps from 5 to 6500 ps to focus on the early TA spectra. The obtained TA spectra are depicted at Figure 4. All spectra exhibit a GSB band at ~ 520 nm and PIA bands at ~ 500 nm and ~ 530 nm. Compared to the TA spectra of 2D perovskites under 530 nm excitation (Figure 3), additional PIA band at ~ 530 nm appears which is due to hot carriers cooling from the high-energy state. By fitting the PIA signal at ~ 530 nm with exponentials, the ultrafast process corresponds to the detailed information of hot carrier relaxation. The normalized kinetic curves based on the exponential fit are presented in Figure 5, and the detailed fitting parameters are given in Table 1. The extracted relaxation times of hot carriers under 400 nm excitation are 0.33 ± 0.02 ps (BA), 0.39 ± 0.02 ps (PEA), 0.34 ± 0.01 ps (TEA), and 0.29 ± 0.03 ps (TMA), respectively. It is clear that the cooling time of hot electrons among the four samples follows the order of $(\text{PEA})_2\text{PbI}_4 > (\text{TEA})_2\text{PbI}_4 > (\text{BA})_2\text{PbI}_4 > (\text{TMA})_2\text{PbI}_4$. In addition, the sub-picosecond time scales for hot carrier cooling of 2D perovskites is consistent with previous reports in the literature.^[30,31]

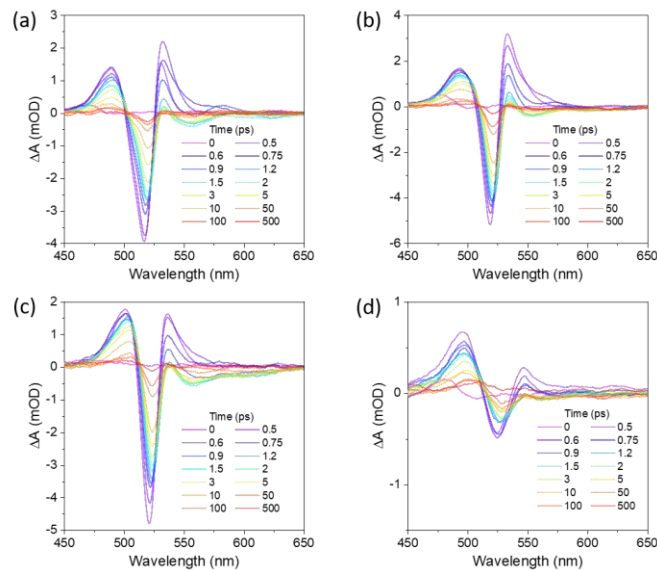


Figure 4: TA spectra under excitation at 400 nm of (a) $(\text{BA})_2\text{PbI}_4$, (b) $(\text{PEA})_2\text{PbI}_4$, (c) $(\text{TEA})_2\text{PbI}_4$ and (d) $(\text{TMA})_2\text{PbI}_4$ at different delay times.

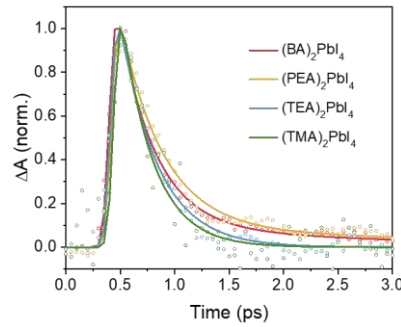


Figure 5: Normalized transient kinetics of 2D perovskites at $\lambda_{probe}=530$ nm.

Table 1: TA kinetics fitting parameters based on exponential model under excitation at 400 nm.

Sample	λ_{probe} (nm)	τ_1 , ps	A_1	τ_2 , ps	A_2
(BA) ₂ PbI ₄	533	0.33 ± 0.02	92%	2.3 ± 0.6	8%
(PEA) ₂ PbI ₄	533	0.39 ± 0.02	92.6%	4 ± 1	7.4%
(TEA) ₂ PbI ₄	536	0.34 ± 0.01	100%	-	-
(TMA) ₂ PbI ₄	543	0.29 ± 0.03	100%	-	-

2.3. Time-resolved photoluminescence (TRPL)

To further verify the modulation of hot carrier relaxation by organic molecules, we measured the PL kinetics by time-resolved photoluminescence (TRPL) under 400 nm excitation. The detailed fitting parameters based on exponential fitting are shown in Table 2. Figure 6 shows the PL kinetic curves of the four samples at different time windows. There is an ultrafast rise process on sub-picosecond time scales in short time windows with rise times of 0.28 ± 0.07 ps (BA), 0.44 ± 0.05 ps (PEA), 0.43 ± 0.05 ps (TEA), and 0.24 ± 0.07 ps (TMA), respectively. As mentioned before, hot carrier relaxation releases excess energy, which leads to an enhancement of the PL intensity. This is accompanied by a corresponding rise process in the TRPL dynamics.^[8,32] Therefore, we attribute the ultrafast process in TRPL to hot carrier cooling, and the order of the relaxation time is (PEA)₂PbI₄ > (TEA)₂PbI₄ > (BA)₂PbI₄ > (TMA)₂PbI₄, which is consistent with the results obtained from TA experiments at the same excitation wavelength.

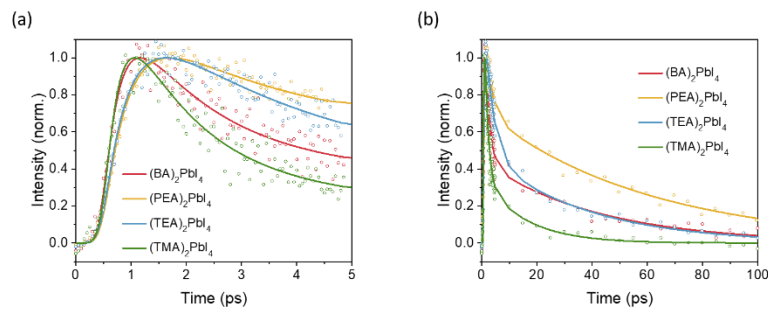


Figure 6: Time-resolved PL of 2D perovskites under excitation at 400 nm within 5 ps and 100 ps time windows.

Table 2: Fitting parameters for TRPL traces of 2D perovskite under excitation at 400 nm.

Sample	λ_{probe} (nm)	t_0 , ps (rise)	A_0	t_1 , ps	A_1	t_2 , ps	A_2
(BA) ₂ PbI ₄	529	0.28 ± 0.07	-98%	1.6 ± 0.3	71.1%	42 ± 8	28.9%
(PEA) ₂ PbI ₄	531	0.44 ± 0.05	-100%	2.1 ± 0.4	49.4%	59 ± 4	50.6%
(TEA) ₂ PbI ₄	537	0.43 ± 0.05	-100%	3 ± 0.5	65.6%	39 ± 6	34.4%
(TMA) ₂ PbI ₄	536	0.24 ± 0.07	-100%	1.3 ± 0.3	78.9%	15 ± 6	21.1%

3. Conclusions

In summary, we present a comprehensive investigation into the hot carrier relaxation dynamics in four different 2D layered $n=1$ perovskites via performing various time-resolved spectroscopic measurements. Transient absorption and time-resolved photoluminescence exhibit that the hot carrier relaxation of 2D perovskites proceeds on sub-picosecond time scales. Additionally, it can be efficiently regulated by component engineering of organic molecules, with the order following $(\text{PEA})_2\text{PbI}_4 > (\text{TEA})_2\text{PbI}_4 > (\text{BA})_2\text{PbI}_4 > (\text{TMA})_2\text{PbI}_4$. Our study highlights the critical role of organic molecules in regulating hot carrier relaxation, which can contribute to further improvements in the device performance of 2D perovskite-based solar cells.

References

- [1] Filip, M.R.; Eperon, G.E.; Snaith, H.J.; Giustino, F. Steric engineering of metal-halide perovskites with tunable optical band gaps. *Nat Commun* 2014, 5, 5757, doi:10.1038/ncomms6757.
- [2] Eperon, G.E.; Stranks, S.D.; Menelaou, C.; Johnston, M.B.; Herz, L.M.; Snaith, H.J. Formamidinium lead trihalide: a broadly tunable perovskite for efficient planar heterojunction solar cells. *Energy & Environmental Science* 2014, 7, doi:10.1039/c3ee43822h.
- [3] Xing, G.; Mathews, N.; Sun, S.; Lim, S.S.; Lam, Y.M.; Gratzel, M.; Mhaisalkar, S.; Sum, T.C. Long-range balanced electron- and hole-transport lengths in organic-inorganic $\text{CH}_3\text{NH}_3\text{PbI}_3$. *Science* 2013, 342, 344-347, doi:10.1126/science.1243167.
- [4] Stranks, S.D.; Eperon, G.E.; Grancini, G.; Menelaou, C.; Alcocer, M.J.; Leijtens, T.; Herz, L.M.; Petrozza, A.; Snaith, H.J. Electron-hole diffusion lengths exceeding 1 micrometer in an organometal trihalide perovskite absorber. *Science* 2013, 342, 341-344, doi:10.1126/science.1243982.
- [5] Ma, L.; Hao, F.; Stoumpos, C.C.; Phelan, B.T.; Wasielewski, M.R.; Kanatzidis, M.G. Carrier Diffusion Lengths of over 500 nm in Lead-Free Perovskite $\text{CH}_3\text{NH}_3\text{SnI}_3$ Films. *J Am Chem Soc* 2016, 138, 14750-14755, doi:10.1021/jacs.6b09257.
- [6] Shi, D.; Adinolfi, V.; Comin, R.; Yuan, M.; Alarousu, E.; Buin, A.; Chen, Y.; Hoogland, S.; Rothenberger, A.; Katsiev, K.; et al. Solar cells. Low trap-state density and long carrier diffusion in organolead trihalide perovskite single crystals. *Science* 2015, 347, 519-522, doi:10.1126/science.aaa2725.
- [7] Guo, D.; Ma, L.; Zhou, Z.; Lin, D.; Wang, C.; Zhao, X.; Zhang, F.; Zhang, J.; Nie, Z. Charge transfer dynamics in a singlet fission organic molecule and organometal perovskite bilayer structure. *Journal of Materials Chemistry A* 2020, 8, 5572-5579, doi:10.1039/c9ta11022d.
- [8] Lin, D.; Ma, L.; Ni, W.; Wang, C.; Zhang, F.; Dong, H.; Gurzadyan, G.G.; Nie, Z. Unveiling hot carrier relaxation and carrier transport mechanisms in quasi-two-dimensional layered perovskites. *Journal of Materials Chemistry A* 2020, 8, 25402-25410, doi:10.1039/d0ta09530c.
- [9] Li, X.; Hoffman, J.M.; Kanatzidis, M.G. The 2D Halide Perovskite Rulebook: How the Spacer Influences Everything from the Structure to Optoelectronic Device Efficiency. *Chem Rev* 2021, 121, 2230-2291, doi:10.1021/acs.chemrev.0c01006.
- [10] Sirbu, D.; Balogun, F.H.; Milot, R.L.; Docampo, P. Layered Perovskites in Solar Cells: Structure, Optoelectronic Properties, and Device Design. *Advanced Energy Materials* 2021, 11, doi:10.1002/aenm.202003877.
- [11] Zhang, F.; Lu, H.; Tong, J.; Berry, J.J.; Beard, M.C.; Zhu, K. Advances in two-dimensional organic-inorganic hybrid perovskites. *Energy & Environmental Science* 2020, 13, 1154-1186, doi:10.1039/c9ee03757h.
- [12] Chen, J.; Lee, D.; Park, N.-G. Stabilizing the Ag Electrode and Reducing J-V Hysteresis through Suppression of Iodide Migration in Perovskite Solar Cells. *ACS Applied Materials & Interfaces* 2017, 9, 36338-36349, doi:10.1021/acsami.7b07595.
- [13] Yang, S.; Chen, S.; Mosconi, E.; Fang, Y.; Xiao, X.; Wang, C.; Zhou, Y.; Yu, Z.; Zhao, J.; Gao, Y.; et al. Stabilizing halide perovskite surfaces for solar cell operation with wide-bandgap lead oxysalts. *Science* 2019, 365, 473-478, doi:10.1126/science.aax3294.
- [14] Zhang, Y.; Liu, Y.; Xu, Z.; Yang, Z.; Liu, S. 2D Perovskite Single Crystals with Suppressed Ion Migration for High-Performance Planar-Type Photodetectors. *Small* 2020, 16, doi:10.1002/smll.202003145.
- [15] Wu, G.; Yang, T.; Li, X.; Ahmad, N.; Zhang, X.; Yue, S.; Zhou, J.; Li, Y.; Wang, H.; Shi, X.; et al. Molecular Engineering for Two-Dimensional Perovskites with Photovoltaic Efficiency Exceeding 18%. *Matter* 2021, 4, 582-599, doi:10.1016/j.matt.2020.11.011.
- [16] Zhang, Y.; Park, N.-G. Quasi-Two-Dimensional Perovskite Solar Cells with Efficiency Exceeding 22%. *ACS Energy Letters* 2022, 7, 757-765, doi:10.1021/acsenenergylett.1c02645.

- [17] Lin, W.; Canton, S.E.; Zheng, K.; Pullerits, T. *Carrier Cooling in Lead Halide Perovskites: A Perspective on Hot Carrier Solar Cells*. *ACS Energy Letters* 2023, 9, 298-307, doi:10.1021/acsenerylett.3c02359.
- [18] Lim, J.W.M.; Giovanni, D.; Righetto, M.; Feng, M.; Mhaisalkar, S.G.; Mathews, N.; Sum, T.C. *Hot Carriers in Halide Perovskites: How Hot Truly? The Journal of Physical Chemistry Letters* 2020, 11, 2743-2750, doi:10.1021/acs.jpcllett.0c00504.
- [19] Li, M.; Fu, J.; Xu, Q.; Sum, T.C. *Slow Hot-Carrier Cooling in Halide Perovskites: Prospects for Hot-Carrier Solar Cells*. *Advanced Materials* 2019, 31, doi:10.1002/adma.201802486.
- [20] König, D.; Casalenuovo, K.; Takeda, Y.; Conibeer, G.; Guillemoles, J.F.; Patterson, R.; Huang, L.M.; Green, M.A. *Hot carrier solar cells: Principles, materials and design*. *Physica E: Low-dimensional Systems and Nanostructures* 2010, 42, 2862-2866, doi:10.1016/j.physe.2009.12.032.
- [21] Wang, G.; Liao, L.P.; Elseman, A.M.; Yao, Y.Q.; Lin, C.Y.; Hu, W.; Liu, D.B.; Xu, C.Y.; Zhou, G.D.; Li, P.; et al. *An internally photoemitted hot carrier solar cell based on organic-inorganic perovskite*. *Nano Energy* 2020, 68, doi:10.1016/j.nanoen.2019.104383.
- [22] O'Keeffe, P.; Catone, D.; Paladini, A.; Toschi, F.; Turchini, S.; Avaldi, L.; Martelli, F.; Agresti, A.; Pescetelli, S.; Del Rio Castillo, A.E.; et al. *Graphene-Induced Improvements of Perovskite Solar Cell Stability: Effects on Hot-Carriers*. *Nano Letters* 2019, 19, 684-691, doi:10.1021/acs.nanolett.8b03685.
- [23] Jia, X.; Jiang, J.; Zhang, Y.; Qiu, J.; Wang, S.; Chen, Z.; Yuan, N.; Ding, J. *Observation of enhanced hot phonon bottleneck effect in 2D perovskites*. *Applied Physics Letters* 2018, 112, doi:10.1063/1.5021679.
- [24] El-Ballouli, A.a.O.; Bakr, O.M.; Mohammed, O.F. *Structurally Tunable Two-Dimensional Layered Perovskites: From Confinement and Enhanced Charge Transport to Prolonged Hot Carrier Cooling Dynamics*. *The Journal of Physical Chemistry Letters* 2020, 11, 5705-5718, doi:10.1021/acs.jpcllett.0c00359.
- [25] Maity, P.; Yin, J.; Cheng, B.; He, J.-H.; Bakr, O.M.; Mohammed, O.F. *Layer-Dependent Coherent Acoustic Phonons in Two-Dimensional Ruddlesden–Popper Perovskite Crystals*. *The Journal of Physical Chemistry Letters* 2019, 10, 5259-5264, doi:10.1021/acs.jpcllett.9b02100.
- [26] Yang, Y.; Ostrowski, D.P.; France, R.M.; Zhu, K.; van de Lagemaat, J.; Luther, J.M.; Beard, M.C. *Observation of a hot-phonon bottleneck in lead-iodide perovskites*. *Nature Photonics* 2015, 10, 53-59, doi:10.1038/nphoton.2015.213.
- [27] Madjet, M.E.; Berdiyrov, G.R.; El-Mellouhi, F.; Alharbi, F.H.; Akimov, A.V.; Kais, S. *Cation Effect on Hot Carrier Cooling in Halide Perovskite Materials*. *The Journal of Physical Chemistry Letters* 2017, 8, 4439-4445, doi:10.1021/acs.jpcllett.7b01732.
- [28] Chen, J.; Messing, M.E.; Zheng, K.; Pullerits, T. *Cation-Dependent Hot Carrier Cooling in Halide Perovskite Nanocrystals*. *Journal of the American Chemical Society* 2019, 141, 3532-3540, doi:10.1021/jacs.8b11867.
- [29] Yang, J.; Wen, X.; Xia, H.; Sheng, R.; Ma, Q.; Kim, J.; Tapping, P.; Harada, T.; Kee, T.W.; Huang, F.; et al. *Acoustic-optical phonon up-conversion and hot-phonon bottleneck in lead-halide perovskites*. *Nature Communications* 2017, 8, doi:10.1038/ncomms14120.
- [30] Yin, J.; Maity, P.; Naphade, R.; Cheng, B.; He, J.H.; Bakr, O.M.; Bredas, J.L.; Mohammed, O.F. *Tuning Hot Carrier Cooling Dynamics by Dielectric Confinement in Two-Dimensional Hybrid Perovskite Crystals*. *ACS Nano* 2019, 13, 12621-12629, doi:10.1021/acsnano.9b04085.
- [31] Yin, J.; Naphade, R.; Maity, P.; Gutierrez-Arzaluz, L.; Almalawi, D.; Roqan, I.S.; Bredas, J.L.; Bakr, O.M.; Mohammed, O.F. *Manipulation of hot carrier cooling dynamics in two-dimensional Dion-Jacobson hybrid perovskites via Rashba band splitting*. *Nat Commun* 2021, 12, 3995, doi:10.1038/s41467-021-24258-7.
- [32] Lin, D.; Ni, W.; Gurzadyan, G.G.; Zhang, F.; Zhao, W.; Ma, L.; Nie, Z. *Trap-free exciton dynamics in monolayer WS₂ via oleic acid passivation*. *Nanoscale* 2021, 13, 20126-20133, doi:10.1039/d1nr05590a.